

# Relocalisation Without Explicit Feature Description in Natural Environments

S. Rolfes and M.J. Rendas  
{rolfes,rendas}@i3s.unice.fr

Laboratoire d'Informatique, Signaux et Systemes de Sophia Antipolis (I3S)  
2000 route des Lucioles BP 121  
06903 Sophia Antipolis  
France

**Abstract**—In this paper we present a novel approach to mobile robot navigation in natural unstructured environments. Natural scenes can be considered as random fields where a large number of individual objects of random shape appear randomly scattered in space. This randomness can be described by statistical models. In this paper we use Random Closed Sets (RCS) to model the random scattering and shape of the objects observed, and base the navigation of a robot on maps of the RCS model's parameters. Contrary to the feature based approach to robot navigation, this environment representation does not require the existence of outstanding objects in the workspace, and is robust with respect to small dynamic changes. We address the problem of estimating the position of a mobile robot assuming that the (statistical) map of the environment is available a priori. We also present an adaptive guidance strategy that autonomously leads the robot to locations where the perceptual observations result in the most efficient reduction of its state uncertainty. Simulations demonstrate the feasibility of our approach.

## I. INTRODUCTION

There is a growing interest in the development of autonomous underwater vehicles (AUV's) for both military and civil applications, such as sea-floor mapping and environment monitoring. AUV's offer a better alternative to human intervention in ocean regions not easily accessible and for long missions. The majority of the navigation systems of AUVs currently in operation rely on the use of long baseline (LBL) arrays of acoustic transponders or to periodic returns to the surface for GPS fixes. These constraints violate the covertness required by some military operations, or imply pre-mission tasks that increase the effective cost of each operation. Moreover, for navigation in coastal areas, the short height of the water column may severely degrade the performance of LBL based systems. An alternative to these approaches is to infer the robot's positions from observation of its environment. A number of robotic research teams have addressed this problem, mostly considering in-door environments.

While stable localisation methods have been proposed for in-door robots, navigation of robots in natural environments is still a challenge. We identify two reasons. First, we are confronted with large scale open environments, that require the ability to navigate to long distances. In the absence of external position information, if pose estimation is based only on dead-reckoning it results in an unbounded increase of the estimation

error. Perceptual information can be used in order to overcome this limitation. The robot creates a map (or uses an existing one), describing the workspace. This map, if it is sufficiently rich, can be used maintain the uncertainty affecting the robot's position bounded during its entire mission. The second point concerns the structure of the environment. Natural scenes are highly unstructured, lacking the geometric type of landmarks (spatially concentrated and simple to describe) on which are based most indoor maps.

It is thus important to assess the question: “*What is the perceptual information that provides the best information for pose estimation ?*”. The most common approaches for localising mobile robots are feature based, see e.g. [1][2]. Other methods use 3D elevation maps [11] (requiring non-flat sea-bottoms), or the use of mosaics [3] based on visual information (requiring flat bottoms). Localisation is basically done by estimating the rigid motion that matches recently observed features to those already contained in the map.

Natural environments have a random appearance. While in structured environments it is possible to identify outstanding features (that can be distinguished from neighbouring ones), this is in general not possible in natural environments, specially when the field of view is limited (myopic perception) as it is the case in underwater robotics. Mismatches due to unstable feature identification, or sparseness of features, violate the basic assumptions behind feature-based maps, and lead to the divergence of the navigation systems that they support.

We propose a novel environment description suitable for environments where identification of salient features is difficult or impossible. Instead of creating a detailed description of the environment as a collection of spatially registered features, we propose a representation by statistical models that capture their local macroscopic characteristics. These characteristics can be (i) the number of objects per unit area, (ii) their spatial distribution, and/or (iii) the distribution of basic local morphological attributes, such as shape, colour or size. We consider this representation as an alternative to other mapping approaches, which, if their underlying conditions are satisfied, yield good results. The major advantage of this representation is that it does not rely on precise knowledge of the position and shape of each individual feature. Mismatch problems are thus eliminated, and the representation is robust to disturbances (small displacement of objects, or shape deformations).

Another important topic on field robotics concerns the efficient use of the environment map. One of its important utilisations is for path planning. An optimal path can be chosen

using a variety of criteria such as minimum path length or minimum uncertainty [13],[14]. For underwater platforms, where the risk of loosing the platform is high, the second criteria is in our opinion crucial [15]. Fully optimal path planning in order to determine a (eventually large) set of intermediate points is computationally heavy, since it imposes search in a high dimensional. In this paper we present a 1-step ahead predictor that guides the robot to the neighboring position where the information provided by the perceptual observations is maximum.

The paper is organised as follows. In section II we motivate our approach, and propose, in section III, the use of RCS models as suitable descriptions of unstructured environments. Sections IV and V give an overview of how RCS models can be used for mobile robot navigation. In section VI we present the information guidance strategy that leads the robot to the most informative areas of the workspace, and in section VII we present preliminary simulation results that validate our approach. We finally draw some conclusions in section VIII.

## II. ENVIRONMENT DESCRIPTIONS

A detailed description of a mobile robot's environment is not required for its navigation. The two basic criteria for the evaluation of mapping approaches are (i) simplicity of coding (*efficiency*) and (ii) robustness of recognition (*performance*). The entities represented in the map depend, naturally, on the nature of the environment in which the robot progresses. The approach that we present here has been motivated by the need of navigating in underwater regions using visual observations of the sea bottom, for which the relevant information is contained in a 2D manifold (the ocean bed). It can, in principle, be extended to other sensors such as sonar, by modeling the random nature of the received signals.

In general, a partition of the robot's workspace can be defined by associating to each point a mark belonging to a limited number of classes. Indoor environments can e.g. be classified into 'corridors', 'walls', 'doors', ... For outdoor environments plausible classes are: 'stones', 'sand', 'tree', etc. This is a rather coarse classification, but still adequate for navigation if the classes are chosen in an appropriate way. This discretised description of the environment can be mathematically represented as the union of compact sets:

$$\Xi = \bigcup_{i=1}^{\infty} (\Xi_i + p_i, m_{i_j}), \quad \Xi_i \in \mathbf{K}, \quad m_{i_j} \in \mathbf{M}. \quad (1)$$

In the equation above  $\mathbf{K}$  is a family of compact sets (set of possible shapes) and  $\mathbf{M}$  is the mark space, designating the class to which the set belongs (describing attributes other than shape).

Without loss of generality, we assume that the center of gravity of the sets  $\Xi_i$  is at the origin. The sum  $\Xi_i + p_i$  denotes the set  $\Xi_i$  translated by the vector  $p_i \in \mathfrak{R}^2$ .

The sets  $\Xi_i$  describe thus the morphological characteristics of the objects (or patches) and  $p_i$  their locations in the workspace. An example is shown in Fig. 1. Fig. 1(a) shows a

raw image of the sea bottom at the Orkney islands in the north of Scotland, where the light regions of the image correspond to dead 'Maerl' (coraline alga). This image shows well the patchy nature of this natural field. The classified version of this image ( $\mathbf{M}$  contains just two classes) is illustrated in Fig. 1(b).

Most of the current approaches to map-based navigation would attempt to describe the individual features of this image (shape and the location of each set  $\Xi_i$ )., If no distinctive features can be detected, as it is the case for this example, the association of recent observations to the map is prone to mismatch, leading to erroneous position estimates. Alternatively, we considering that the patches form a random pattern, which can be formally modelled using the notion of *random closed sets* (RCS), and map just the statistical characteristics of the sets  $\{p_i\}$  and  $\{\Xi_i\}$ .

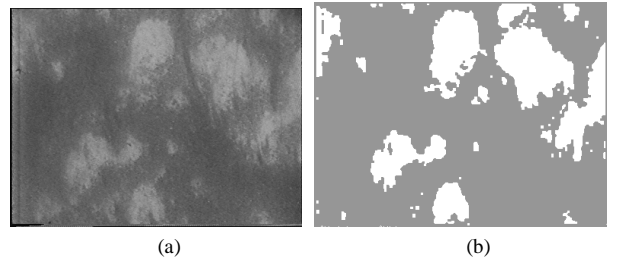


Fig. 1 Image of a 'Maerl' field, taken in the North of Scotland. (b) the segmented image showing the random distribution of the patches.

## III. MODELLING OF SCATTERED OBJECTS AS RANDOM CLOSED SETS

Random closed sets are mathematical models appropriate for modelling of random-like patterns. They have been frequently used in biological and physical studies in order to analyse natural patterns. Good introductions to this formalism can be found in [4][5].

A *random closed set* (a collection of randomly shaped compact sets, as given by equation (1)) is a doubly stochastic process, also called germ-grain model. A first random point process describes the spatial location of objects (germs), denoted by  $p_i$  in equation (1), at which realisations of a second stochastic process (grains) determine the local morphology of the field, i.e. the characteristics of the sets  $\Xi_i$ . The intersection between distinct patches can be non empty. The distribution of the germs can, for example, be clustered, structured or uniformly distributed, see Fig. 2.

We assume that the counting measure  $\mu$  associated to the point process (germ model) is a member of a parameterised family of distributions  $G_p$ :

$$\mu \in G_p = \{\mu_\lambda : \lambda \in \Gamma\},$$

where  $\Gamma$  is a compact set. The vector  $\lambda$  is the collection of parameters that determine the statistical distribution of the locations  $p_i$ . The shape process (grain model) constrains the

set of possible elementary shapes (e.g. to discs of random radius, lines of random orientation or mixtures of them). Similarly to the germ process, we consider that the distribution of the shapes can be parameterised by a finite number of parameters  $\gamma$ , such that

$$\kappa \in G_{\Xi_0} = \{\kappa_\gamma, \gamma \in \Lambda\},$$

where  $\kappa$  is a probability measure over the space of possible shapes,  $\Lambda$  is a compact set and  $\Xi_0$  is a random shape. Different model types can be obtained by considering distinct pairs of families  $G_p, G_{\Xi_0}$  (for instance, for  $G_p$ : homogeneous Poisson point process, regular pattern, etc., and for  $G_{\Xi_0}$ : discs whose radii are uniformly distributed in an interval, line segments of random length and orientation, etc.).

The random closed set model is thus given by the model type  $M_{i,j} = (G_p^{(i)}, G_{\Xi_0}^{(j)})$ . A particular model  $M \in M_{i,j}$  is specified by the parameter vector  $\theta = (\lambda, \gamma)$ ,  $M(\theta) = \{\mu_\lambda, \kappa_\gamma\}$ , where  $\mu_\lambda \in G_p^{(i)}$  and  $\kappa_\gamma \in G_{\Xi_0}^{(j)}$ .

The aim of the theory of random closed sets is to determine the model type  $M_{i,j}$  and the model parameter  $\hat{\theta} = (\hat{\lambda}, \hat{\gamma})$ , such that an observed scene (inside an observation window (OW) of size  $\nu(OW)$ , where  $\nu(\cdot)$  is the Lebesgue measure) is a typical realisation of the random closed set model  $M(\theta) \in M_{i,j}$ .

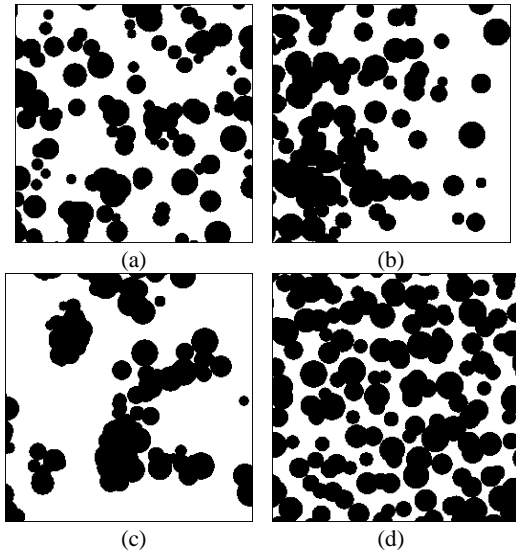


Fig. 2 Example of RCS models. with different point processes. (a) isotropic Boolean model, (b) anisotropic Boolean model, (c) clustered distribution and (d) regular distribution of the grains.

It is often difficult to obtain direct estimates of the counting measures and of the morphological characteristics of the sets  $\Xi_i$  from classified images, especially when the elementary grains  $\Xi_i$  may overlap, as illustrated in Fig. 2. Estimation of the distributions of the germ and the grain processes by direct identification of each individual shape is in these cases impossible.

We exploit here an important property of random closed sets [6], stating that the distribution of any general random

closed set is uniquely determined by the **hitting capacity** which is, for each compact set  $K$ , the probability that the intersection of  $K$  with the RCS  $\Xi$  is not empty:

$$T_{\Xi}(K) = P(\Xi \cap K \neq \emptyset), \forall K \in \mathcal{K} \quad (2)$$

The important fact is that knowledge of the hitting capacities for all  $K \in \mathcal{K}$  is *equivalent* to knowledge of the model parameter  $\theta$  (assuming the model type to be known). In the case of isotropic models ( $\theta$  is independent of the location and orientation of the observer) we know that  $T_{\Xi}(K) = T_{\Xi}(K+p)$ . Under the assumption that the RCS model is locally isotropic (inside the observation window WO) we can obtain empirical estimates of the hitting capacities from classified images.

For obvious reasons (limited computational capacities) we are able to estimate the hitting capacities only for a finite collection of compact sets  $K^n = \{K_1, \dots, K_n\}$ , which we call structuring elements [7].

For some model types we can find analytical forms of equation (2), allowing us to compute the hitting probabilities in terms of the model parameters  $\theta$ . This is the case for the well studied **Boolean model**. The germ process is a Poisson point process, determined by the intensity parameter  $\lambda$ , and the grains are i.i.d. realisations of compact sets. The hitting capacity for Boolean models can be shown (see [4]) to be

$$T_{\Xi}(K) = 1 - \exp(-\lambda E_{\kappa}(\nu(\Xi_0 \oplus K))),$$

where  $\oplus$  is the Minkowski-addition  $A \oplus B = \{a+b, \forall a \in A, b \in B\}$ ,  $E_{(\cdot)}$  is the statistical expectation operator with respect to the measure  $\kappa$  of the shape process and  $\tilde{K} = \{-x, x \in K\}$ . In this presentation of our approach to mobile robot. navigation we concentrate on Boolean models. Ongoing work concerns characterisation of other types of random closed set models as those illustrated in Fig. 2. Example of RCS models. with different point processes. (a) isotropic Boolean model, (b) anisotropic Boolean model, (c) clustered distribution and (d) regular distribution of the grains., in particular clustered models, which seem good candidates to describe some kinds of natural scenes.

In general, the shape and distributions of the objects present change throughout the workspace, induced by varying temperature, soil fertility, ocean current, etc. If these variations are abrupt, we can partition the workspace into disjoint areas  $A_k$  (see Fig. 3), whose macroscopic characteristics are described by different types of statistical models  $M_{i_k, j_k}(\theta)$ :

$$Workspace = \bigcup_{k=1}^{\infty} A_k, A_k \rightarrow M_k(\theta) = (\mu_{\lambda}^{(i)}, \kappa_{\gamma}^{(j)}),$$

where  $M_k(\theta)$  is the model associated to area  $A_k$ . To model smooth variations of the field inside each region  $A_k$ , we let the model parameter  $\theta$  depend on the location  $x$

$$\text{Map: } x \rightarrow \theta(x) = (\lambda(x), \gamma(x)) \quad x \in A_k. \quad (3)$$

The approach to navigation of robots in natural environments proposed here considers that the map given in the previous equation has been learned by (or given a priori to) the robot, i.e., the robot knows the partition  $\{A_k\}$  and the piecewise continuous vector field defined by equation (3).

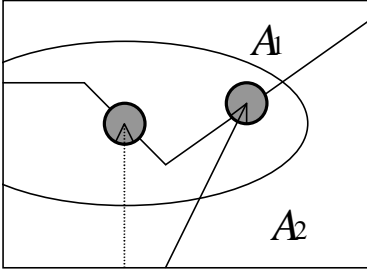


Fig. 3 The workspace is segmented in two areas. If the robot passes the boundary, localisation is possible. In the case of large pose uncertainty the set of possible locations (all along the boundary), is very large.

#### IV. MOBILE ROBOT NAVIGATION BASED ON RCS MODELS

We address now the problem of using the map defined in the previous section to estimate the robot location. Local observations provide useful information for localisation only inside anisotropic areas of the RCS (the model parameter is a function of the location). An anisotropic field is illustrated in Fig. 2(b). In this case the pose error can be permanently corrected and positioning uncertainty is kept bounded. Accuracy of the localisation depends on the informativeness of the field: strong variations of the field result in more accurate pose estimates since distinction between different locations inside the area is more accurate. If the areas  $A_k$  are isotropic, localisation is only possible when the robot observes a boundary between adjacent areas, indicated by an abrupt change of the model parameter or of the model type (Fig. 2(a) illustrates an isotropic field). The problem is that during navigation inside isotropic areas the pose error grows considerably leading to a large uncertainty when the robot reaches the boundary, and ultimately resulting in a large set of possible true locations along the boundary (ambiguity). Most approaches to position estimation for mobile robots use Extended Kalman filters, and must thus assume that the observations are differentiable with respect to the robot's state. Navigation between adjacent areas requires in this case a first symbolic association step, prior to actual observations filtering. We propose a method that does not rely on this two step decomposition.

We first formulate the general framework of the Bayesian approach to localisation. Assume that the dynamic model of the robot's state  $X_k$  and the observation model are known:

$$X_{k-1} = f(X_{k-1}, u_{k-1}) + w_{k-1}, \quad (4)$$

$$Y_k = h(X_k) + v_k, \quad (5)$$

where  $f(\cdot, \cdot)$  and  $h(\cdot)$  are known (non-linear) functions,  $f: C \times U \rightarrow C$ ,  $h: C \rightarrow E$ , where  $C$  is the configuration space of the robot's state,  $U$  is the space of the control input,  $u_k$ ,  $E$  is the space of the perceptual observations and  $w_{k-1}, v_k$  are uncorrelated, zero-mean white noises. The optimal MMSE estimate of the robot's state given the past observations  $Y^k = \{Y_1, \dots, Y_k\}$  is given by the conditional mean

$$\hat{X}_k = \int_C X_k p(X_k | Y^k) dX_k,$$

where  $p(X_k | Y^k)$  is the posterior density, which can be recursively updated by alternating prediction and filtering steps:

$$p(X_{k-1} | Y^{k-1}) \xrightarrow{\text{Pred.}} p(X_k | Y^{k-1}) \xrightarrow{\text{Filt.}} p(X_k | Y^k). \quad (4)$$

The prediction step (convolution) propagates the probability distribution in the state space according to the dynamic model. If  $Y_k$  is the output of a memoryless observer, the filtering step (pointwise multiplication) computes

$$p(X_k | Y^k) \propto p(X_k | Y^{k-1}) p(Y_k | X_k).$$

The observations  $Y_k = (D_k, Z_k)$  contain proprioceptive observations  $D_k$  (velocity, heading, ...) and measures  $Z_k$ , obtained using perceptual sensors (vision, sonar, ...). The measures  $Z_k$  are in our case estimates of the hitting capacities for a set of structuring elements  $K^n$ . These estimates are obtained directly from the classified images:  $Z_k = \{\hat{T}_k = \{\hat{T}_k(K_1), \dots, \hat{T}_k(K_n)\}\}$ . If we assume that, given the robot's state, the proprioceptive and the perceptual observations are uncorrelated we obtain:

$$p(Y_k | X_k) = p(D_k | X_k) p(\hat{T}_k | \theta(X_k)),$$

since the observations  $Z_k$  depend on  $X_k$  only through the parameters of the RCS model at that point. In order to use an optimal filter we need to know the conditional density  $p(\hat{T}_k | \theta(X_k))$ , which is, in general, not Gaussian.

The equations above define the general framework of navigation using a Bayesian approach. In the actual state of the work we are restricted to RCS models that are locally (inside the observation window) isotropic. For these models we are able to identify the density  $p(\hat{T}_k | \theta(X_k))$  with a binomial distribution.

An estimate  $\hat{T}$  of the hitting capacities can be obtained by placing each structuring element of  $K^n$  at  $N$  (sampling number) random positions  $\{p_1, \dots, p_N\}$  inside the observation window and evaluating each time the event:  $K_j$  hits (or not) the random field  $\Xi$ . If the events are mutually independent, the probability of the number of hits  $H$  follows a binomial distribution:

$$p(H|N) = \binom{N}{H} \hat{T}(K_j)^H (1 - \hat{T}(K_j))^{N-H},$$

where  $\hat{T}(K_j) = \hat{H}/N$  is the estimated hitting capacity ( $\hat{H}$  is the observed number of hits). The variance of  $p(H|N)$  is  $\sigma_H^2 = N\hat{T}(K_j)(1 - \hat{T}(K_j))$ .

In order to guarantee that the individual hitting events are mutually independent it is important to choose an appropriate sampling number  $N$ . This number depends on the size of the observation window, the structuring element and on the RCS model. The determination of the optimal number is still an ongoing problem. Note however that the number of hits follow a binomial distribution for  $N$  smaller than the optimal value. For large  $N$  the binomial distribution can be approximated by a normal distribution (see Fig. 4):

$$p(\hat{T}|\theta(X_k)) \cong \mathcal{N}(\hat{H}/N, \hat{T}(1 - \hat{T})/N),$$

where  $\mathcal{N}(x, A)$  is the normal law with mean  $x$  and covariance  $A$ .

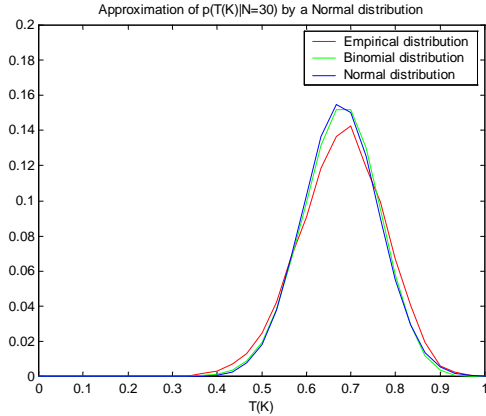


Fig. 4 Binomial distribution of the number of hits and its approximation by a normal distribution.

## V. IMPLEMENTATION OF THE OPTIMAL FILTER

Direct computation of the prediction (convolution) and filtering (pointwise multiplication) steps is in practice not feasible. We saw in the previous section that the observation noise (for locally isotropic models) is well approximated by a normal distribution. Under the assumption that the noises  $w_k, v_k$  of equations (4) and (5) are zero mean and Gaussian with covariances  $Q$  and  $R$ , respectively, and linearising the state and observation model around the current estimate of the robot's state an approximation of the optimal non-linear filter is given by the standard Extended Kalman Filter (EKF). The linearised state and observation models are given by:

$$\begin{aligned} X_k &\cong f(X_{k-1}, \mu_{k-1}) + \dot{F}_k (X_{k-1} - X_{k-1|k-1}) + w_{k-1}, \\ Y_k &\cong h(X_{k|k-1}) + \dot{H}_k (X_k - X_{k|k-1}) + v_k, \end{aligned}$$

where  $\dot{F}_k = \left. \frac{\partial f(\dots)}{\partial X} \right|_{X_{k-1|k-1}, \mu_{k-1}}$  and  $\dot{H}_k = \left. \frac{\partial h}{\partial X} \right|_{X_{k|k-1}}$ .

This approximation is based on the assumption that at each step the estimation error is small. To prevent filter divergence, the linearisation must be a good approximation over the entire uncertainty domain, which is the case when the robot is moving in informative anisotropic areas. However, navigation in isotropic areas leads to a considerable growth of the uncertainty of the robot's state and linearisation of the non-linear model may artificially shrink the estimated uncertainty of the position estimates, creating the possibility that the EKF diverges. As we mentioned before, this is particularly important when the robot reaches the boundary of adjacent areas after having crossed an isotropic area where consideration of the linearised model leads to a null gain for perceptual information.

In [9] we proposed an approximation of the optimal non-linear filter by a Gaussian Mixture Model (GMM). We assume that the posterior density of the robot's state at time  $k-1$  is Gaussian. We approximate the prediction density of equation (4) by a Gauss mixture:

$$p(X_k|Y^{k-1}) \cong \sum_{i=1}^{N_k} s_{k-1}^i p(X_k|Y^{k-1}), \quad \sum_{i=1}^{N_k} s_{k-1}^i = 1,$$

where the prediction density for each term is normal distributed with mean  $x_{k|k-1}^i$  and covariance  $\Sigma_{k|k-1}^i$ . Each term is multiplied by a scaling parameter  $s_{k-1}^i$ .

We assume that the number  $N_k$  and the mean and variance of the terms are chosen such that linearisation of the state space model around each term is valid inside the principal support of each component [9]. Application of the filtering equation results then in a Gaussian mixture with the conditional mean [9]:

$$X_{k|k} = \sum_{i=1}^{N_k} s_k^i X_{k|k}^i.$$

The updated scaling parameter after filtering,  $s_k^i$ , are given by:

$$s_k^i = s_{k-1}^i C_k^i \frac{C_k^i}{\sum_{l=1}^{N_k} s_{k-1}^l C_k^l}; \quad C_k^i = \frac{|\Sigma_{k|k}^i|}{|R| |\Sigma_{k|k-1}^i|} \exp\left(-\frac{1}{2} z_k^i T S_k^{i-1} z_k^i\right),$$

where  $z_k^i = Y_k - h(X_{k|k-1}^i)$  are the innovations of each term and

$$S_k^i = \dot{H}_k^i T \sum_{l=1}^{i-1} \dot{H}_{k|k-1}^l \dot{H}_k^l + R$$

their innovation matrices. The principal result is that each component can be propagated by an EKF, and repeated application of the prediction and filtering step results always in a Gaussian mixture. The scaling parameter depends strongly on the innovations and as a consequence, terms for which the predicted observations (hitting capacities) correspond well to the true observations (small innovations) are reinforced, otherwise they loose importance and will not contribute significantly to the posterior density. When crossing a boundary between adjacent areas, the terms on the ‘correct’ side are reinforced while all other loose importance, resulting in a concentration of the density mass around the true location of the vehicle.

In the current implementation of the filter we trigger the mixture model when the linearisation is no longer valid over the entire domain of uncertainty. For navigation between isotropic areas this is the case when a boundary lies inside the significant support of the uncertainty domain. In order to reduce the computational complexity of the filter (depending linearly on the number of terms), we eliminate spurious terms (the scaling parameter falls below a given threshold) and fuse close terms. If all but one term are eliminated we return to the simple EKF.

## VI. OPTIMAL OBSERVATION STRATEGY

An important issue on autonomous navigation is to choose a trajectory that reduces the uncertainty of the robot at its destination. This corresponds to the problem of defining a sequence of control inputs  $U_k^{k+M} = \{u_k, \dots, u_{k+M}\}$  that moves the robot through  $M$  intermediate positions between the current position and the destination position, such that the uncertainty at the destination is mimised. Such a path can be obtained by a recursive  $M$ -step predictor with the constraint that the final position must be the destination. Here we limit the problem to a 1-step ahead predictor that drives the robot to the next position where the information gain is maximum.

It is known [12] that the estimate of the EKF,  $\hat{X}_{k|k}$ , (assuming the validity of the linearisation) minimises the mean square error for a given control input  $u_k$ :

$$J_k(u_k) = \int_C (X_{k|k} - X_k)^T (X_{k|k} - X_k) p(X_k | Y^k) dX_k.$$

We want to find the control input  $u_k^*$  that minimises the above function:

$$u_k^* = \arg \min_{u_k \in U} (J_k(u_k)).$$

For the Gaussian mixture,

$$\begin{aligned} J_k(u_k) &= \sum_{i=1}^{N_k} s_k^i \int_C \|X_{k|k} - X_k^i\|^2 p_i(X_k^i | Y^k) dX_k^i \\ &= \sum_{i=1}^{N_k} s_k^i \|b_k^i\|^2 + \sum_{i=1}^{N_k} s_k^i \int_C \|X_{k|k}^i - X_{k|k}\|^2 p_i(X_k^i | Y^k) dX_k^i, \end{aligned}$$

where  $b_k^i = X_{k|k}^i - X_{k|k}$ .

The first term of the previous equation reflects the error due to the distribution of the terms and the second the uncertainty of each term, given by covariance matrix  $\Sigma_{k|k}^i$ .

In our implementation we defined a finite set of control inputs that guide the robot to a dense set of positions the region ahead of it. For each control input we evaluate the mean square error and choose the control input that leads to the minimum error. The computation of the mean square error depends strongly on the innovations, and thus on the perceptual observations (not know), via the scaling parameters and the estimates of each term. In order to evaluate the mean square error we predict the perceptual observations (the hitting capacities) as

$$T(K_j) = \int_C T_{\theta(X_k)}(K_j) p(X_k | Y^{k-1}) dX_k,$$

for each structuring element  $K_j \in K^n$ .

## VII. RESULTS

In [10] we demonstrated navigation of a mobile robot inside anisotropic areas. The approximation of the optimal filter by an EKF was valid, since the uncertainty of the robot was maintained small during the entire trajectory. The linearisation around the estimated state was thus valid over the principal uncertainty support, enabling application of the EKF.

Here we discuss navigation between isotropic areas, which does not allow permanent localisation. We simulated the navigation of an underwater robot equipped with proprioceptive sensors (compass and speed sensor) that are used for dead-reckoning, and with a camera pointing at the sea bottom. The robot moves at a constant altitude above the sea bed. The workspace is divided into two areas. In each area, The RCS model is an isotropic boolean model, where the grains are compact discs whose radius is uniformly distributed in an interval  $r \in (r_1, r_2)$ . The intensity of the Poisson point process is constant inside each area and changes abruptly at their frontier. The workspace for  $\lambda_1=0.002, \lambda_2=0.001$  ( $\lambda_i$  is the intensity of the point process in area  $A_i$ ) is shown in Fig. 5 (only the locations of the grains are indicated), along with the location of the robot and the position estimate (obtained by an EKF), indicated by a large cross (with a large error, resulting from the previous dead-reckoning period). The ellipse

indicates the initial uncertainty (predicted by an EKF) and the square the area that is observed by the camera.

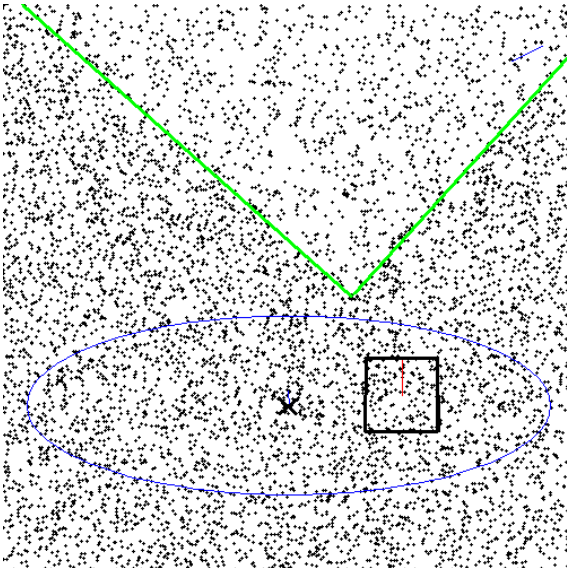


Fig. 5 Realisation of a random field, where the change of the intensity of the point process defines the frontier (indicated by the segments) between the areas.

A simulated (non-observed) ocean current perturbs the nominal trajectory of the robot, resulting in an important drift between the true position and its dead-reckoning estimate. Throughout the trajectory, that was chosen in order to guarantee that the frontier is crossed, images are acquired at regular time intervals. The perceptual observations are empirical estimates of the hitting capacity  $Z_k = \{\hat{f}_k(K_i)\}$  for a single structuring element (square of side length 10) that are directly obtained from the images based on a fixed number  $N = 30$  of samples.

The Gaussian mixture is triggered when the boundary lies inside the significant support of the uncertainty of the EKF estimate. The uncertainty support ( $3\sigma$ ) is indicated by the thin ellipsis. The terms of the Gaussian mixture are indicated in Fig. 6 by the plus signs and the boundary of the principal support (coverage 99%) of the posterior density is indicated by the thick line (initially Gaussian). The mean of the mixture (the Minimum Mean Square Error estimate) is shown as a large circle and the trajectory (in the subsequent figures) is shown as a dashed line.

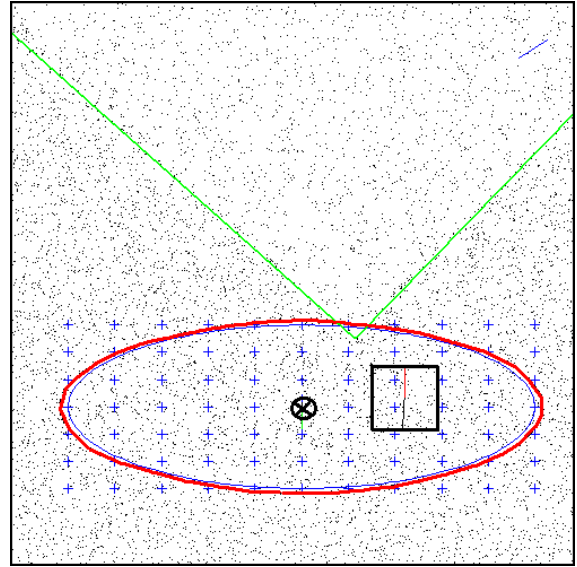


Fig. 6 Creation of the Gaussian Mixture Model. The terms are indicated by the plus signs.

At each iteration the robot searched for the optimal control input, restricted to those driving the robot inside a cone in front of the robot. The angular aperture of the cone was restricted to 90 degrees and the most distant position was at 70 (the size of the observation window, indicated by the large square is  $260 \times 260$ ). It should be noted that due to the stochastic nature of the observations (see figure Fig. 4 for the uncertainty of the observed hitting capacities), the effective uncertainty reduction does not coincide with the predicted one. Fig. 7 shows, however, that the effective mean square error follows well the predicted error throughout the whole trajectory.

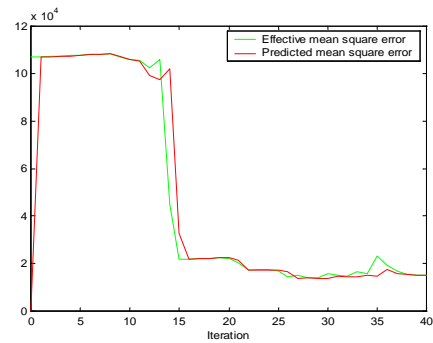


Fig. 7 The effective mean square error after application of the optimal action is close to the predicted error.



Fig. 8 Observations of the scene (a) inside area 1, (b) on the boundary, (c) inside area 2.

The progression of the robot is illustrated in Figures 8,9 and 10 for three iterations. The typical images of the field (inside area 1, on the boundary and inside area 2) obtained by the simulated camera are indicated in Fig. 8. Due to the optimal control input the robot is driven in direction of the boundary (Fig. 9), where the information gain of the perceptual observations is maximal. Upon reaching the boundary, the uncertainty reduction, illustrated by Fig. 10 and Fig. 7 (around iteration 15), is considerable. The robot maintains then its trajectory along the boundary (in an oscillating manner), as illustrated in Fig. 11. The uncertainty (perpendicular to the boundary) remains bounded. This is not the case for the uncertainty in the direction of motion of the robot. In order to reduce this uncertainty, the best action to be performed is to turn and to go back to the corner. In the actual implementation we restricted the control to movements in front of the robot (taking roughly into account the dynamic constraints of the vehicle), precluding thus backward motion. However there is no conceptual difficulty in predicting the optimal position in a circular region around the robot and perform local path planning to drive the robot to that position.

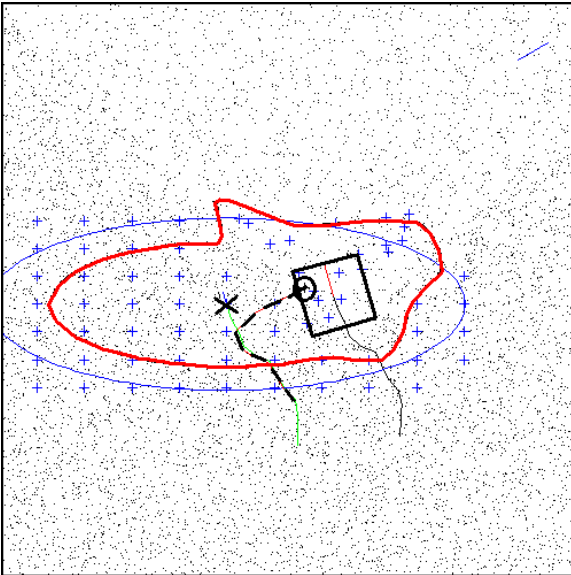


Fig. 9 The simulated robot is located at the boundary. The estimate of the gaussian mixture filter can exploit the perceptual observations, while the EKF estimate predicts a null gain

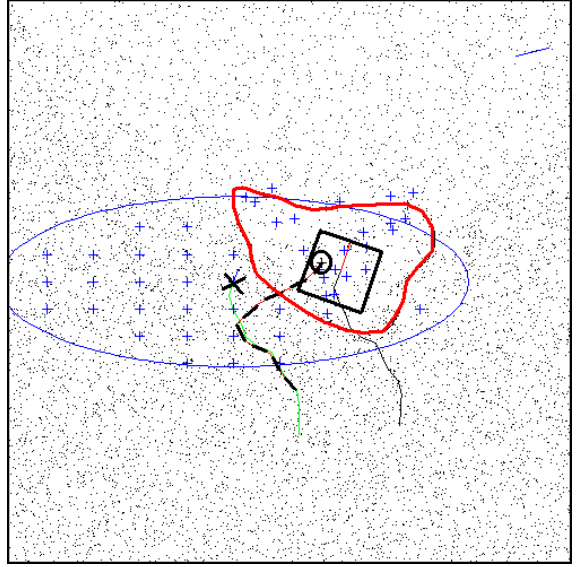


Fig. 10 The simulated robot passed entirely to the second area (lower intensity). At this step (compare with the previous figure) the uncertainty reduction is most significant. The scaling parameter of the terms still located in the area with the larger intensity is close to 0 and can be removed from the mixture.

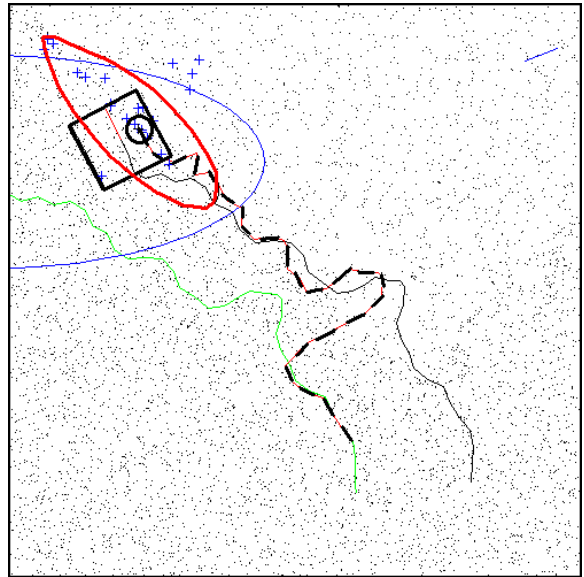


Fig. 11 The robot maintains its trajectory on the boundary, since it provides the best information. The pose error of the EKF estimate has grown throughout the whole trajectory (the pose estimate is no longer inside the figure).

## VIII. CONCLUSIONS

In this paper we propose a novel environment description for robot navigation, using the formalism of random closed set models. These models capture the principal characteristics of natural environments. The approach was motivated by the fact that identification of outstanding features, on which the majority of existing approaches to robot localisation is based, is not always possible. Description by statistical models does not rely on the identification of outstanding features and

knowledge of their exact location (or shapes) is not required, resulting in increased robustness with respect to small changes.

We present approximate expressions that enable definition of an approximation of the Bayesian estimator of the robot state for RCS models. We addressed the problem of ambiguity in the workspace, precluding the use of a simple EKF, when uncertainty of the estimated pose is very large. An approach that is related to multiple hypothesis, the Gaussian mixture model, is proposed and its feasibility is demonstrated by simulation results. In order to use the RCS map in an efficient way we propose an observation strategy that drives the robot to locations inside the workspace where the information provided by the perceptual observations results in the most significant reduction of uncertainty.

A series of open problems must still be studied more thoroughly. In particular, we need to handle more complex RCS models which are good candidates to describe real environments. We focus our attention especially on clustered or regular distributions of the grains. Approximate analytical expressions for the hitting capacities need to be found for these models. Another issue concerns the Gaussian mixture model. In particular we need to add additional terms (a split of significant ones) to the mixture in the case where the linearisation is no longer valid. Close terms can on the contrary be fused in order to reduce the complexity of the filter. Fusion must not result in a decrease of uncertainty. Finally the problem of joint mapping and localisation for this kind of environment representations must be addressed in order to realise fully autonomous progression of a robot in a priori unknown environments: the robot must be able to simultaneously estimate the map (the model type along with the model parameter) and its position, using the autonomously created map.

#### IX. ACKNOWLEDGMENT

This work has been partially funded by the European Union through the IST project SUMARE (IST-1999-10836, Survey of Marine Resources) and the Esprit/LTR project NARVAL (LTR-20185, Navigation of Autonomous Robots via Active Environment Perception).

#### X. REFERENCES

- [1] H.J. Feder, J.J. Leonard, and C.M. Smith, "Adaptive Mobile Robot Navigation and Mapping" *Int Journal of Robotics Research*, July 1999.
- [2] J.A. Castellanos, J.M. Martinez, J. Neira, J.D. Tardos, "Simultaneous Map Building and Localisation for Mobile Robots: A Multisensor Fusion Approach" " in *IEEE Proc. Of the Int Conf. On Robotics and Automation*, May. 1998.
- [3] N. Gracias, "Application of robust estimation to computer vision: Video mosaics and 3-D reconstruction", Master thesis at Universidade Tecnica de Lisboa, 1997
- [4] D. Stoyan, W.S. Kendall, J. Mecke, "Stochastic Geometry and its Applications", John Wiley & Sons, 1995.
- [5] O.E. Barndorff-Nielsen, W.S. Kendall, M.N.M. van Lieshout, "Stochastic Geometry, Likelihood and Computation", Chapman & Hall/CRC 1999.
- [6] G. Matheron, "Random Sets and Integral Geometry", John Wiley & Sons, New York 1982.
- [7] J. Serra, "Image Analysis and Mathematical Morphology", Academic Press, New York, 1982.
- [8] J. Rissanen, "Statistical Complexity in Statistical Enquiry", World Scientific, 1989..
- [9] J.M. Rendas, S. Rolfes, "Using Non-linear Filtering Techniques for Robot Localisation in Sparse Environments using Perceptual Sensors", Proc. Of the 7<sup>th</sup> Int. Symposium on Intelligent Robotic Systems, Coimbra, Portugal, July 1999, pp 429-438.
- [10] S. Rolfes, J.M. Rendas, "Statistical environment representation for navigation in natural environments", Proc. Of the 9<sup>th</sup> Int. Symposium on Intelligent Robotic Systems, Toulouse, France, July 2001.
- [11] S. Lacroix, I.K. Jung, A. Mallet, "Digital Elevation Map Building from Low Altitude Stereo Imagery", Proc. Of the 9<sup>th</sup> Int. Symposium on Intelligent Robotic Systems, Toulouse, France, July 2001
- [12] A. Gelb, "Applied Optimal Estimation", Mit Press, 1974.
- [13] H. Takeda, C. Facchinetti, J.C. Latombe, "Planning the Motion of a Mobile Robot in a Sensory Uncertainty Field", IEEE Transactions on Pattern Analysis and Machine Intelligence, vol. 16, October 1994.
- [14] R. Bauer, "Active manoeuvres for supporting the localisation process of an autonomous mobile robot", Robotics and Autonomous Systems, vol. 16, 1995.
- [15] J.M. Rendas, S. Rolfes, "Learning safe navigation in uncertain environments", Robotics and Autonomous Systems, vol. 31, 2000.